Supplementary Information

Potential for Electricity Generation from Renewable Resources and Levelized Cost of Electricity (LCOE)

Electrical energy can be generated from renewable resources such as solar, wind, hydropower, geothermal, tidal and wave energy. Currently, most of these resources have the potential to meet the worldwide demand of electricity and they contribute to the total generation of electricity with only a small fraction of their actual potential. Hydroelectric power is the most widely used form of renewable energy and developed to about 16% of its potential.
Supplementary figure S1 compares the annual potential and actual annual production of electrical energy from renewable energy resources. Only tidal energy is not capable of providing a significant amount of the worldwide consumption of electrical energy. The disparity between potential and production is most striking for wave energy: While capable of providing enough energy to meet the world demand of electricity, the current amount of electricity generation from waves is negligible.

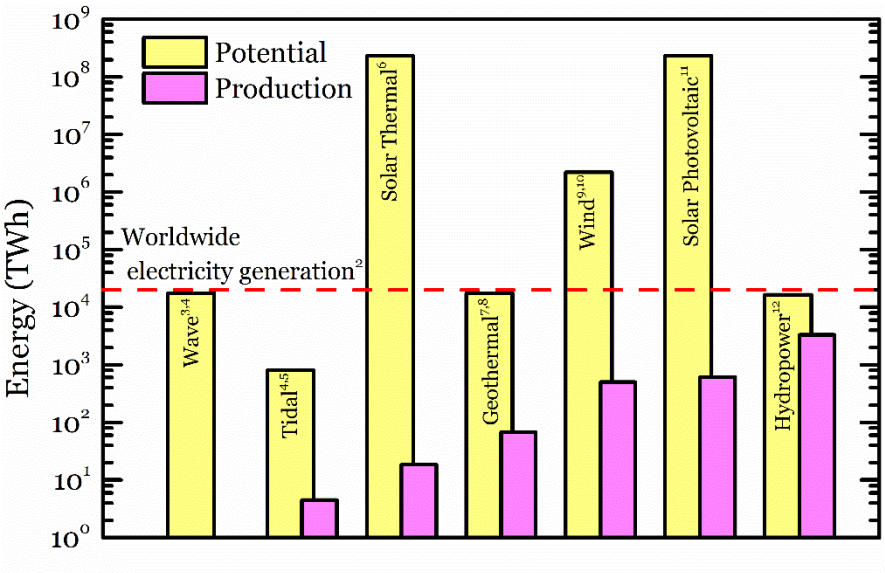

Supplementary Figure S1 | Availability of renewable sources (References are given by superscripted numbers) a) The worldwide potential and production of electrical energy from different renewable sources. The red dashed line marks the world consumption in the year 2009. The total potential of solar energy was calculated by multiplying the average annual solar irradiation[1] ($168\ W/m^2$) with a total landmass ($148 \times 10^6 km^2$).[2–12]

The LCOE describes at what price each kWh of generated electricity from a given project must be sold to break even over the lifetime of the project. The LCOE varies for different technologies and energy resources.

A general calculation of LCOE involves the knowledge of six quantities for each year t of operation: annual investements (so called capital expenditure $CAPEX(t)$), annual maintenance (so called operational expenditure $OPEX(t)$), annual fuel cost ($FUEL(t)$), annual renumeration of generated electricity ($EGEN(t)$), annual discount rate ($r(t)$) and the lifetime of the device (T) in years. These quantities are combined to calculate the LCOE in the following equation

$$LCOE = \frac{\sum_{t=1}^{T} \frac{\mathrm{CAPEX}(t) + \mathrm{OPEX}(t) + \mathrm{FUEL}(t)}{[1+r(t)]^t}}{\sum_{t=1}^{T} \frac{\mathrm{EGEN}(t)}{[1+r(t)]^t}} \quad (S\,1)$$

A simplification is achieved by the assumption that all investments are made in the first year ($\mathrm{CAPEX}(t=0) = \mathrm{CAPEX}_{\mathrm{total}}$ and $CAPEX(t \neq 0) = 0$) and all other quantities are constant over the whole lifetime

$$LCOE = \frac{\mathrm{OPEX} + \mathrm{FUEL}}{\mathrm{EGEN}} + \frac{\mathrm{CAPEX}_{\mathrm{total}}}{\mathrm{EGEN}} \frac{r\,(1+r)^T}{(1+r)[(1+r)^T - 1]} \quad (S\,2)$$

Evaluating the LCOE requires deep knowledge of technical limits, the jurisdiction which applies (fees, taxes), financial environment (interest rates, availability of capital and expected inflation), government support, public support, and much more[13,14]. For this reason we base our analysis on that of Previsic, Bedard and McGowin et al.[13,15,16] who broke down the cost centers for the LCOE of a rigid wave energy converter (Pelamis) (see supplementary fig. S2 a). Pelamis is a rigid wave energy converter (WEC), see supplementary fig. S2 b), comprising steel tubes floating on the surface which move against each other due to wave motion with hinges transmitting the absorbed mechanical energy to power take-off systems. Addressing each cost center individually, we assess the differences between rigid and soft WECs to obtain an estimate for their LCOE. Soft WECs comprise an elastomer tube filled with pressurized water[17]. The walls of the tube are built as dielectric elastomer generators which directly convert mechanical deformation energy of the wall into electrical energy (supplementary fig. S2 c).

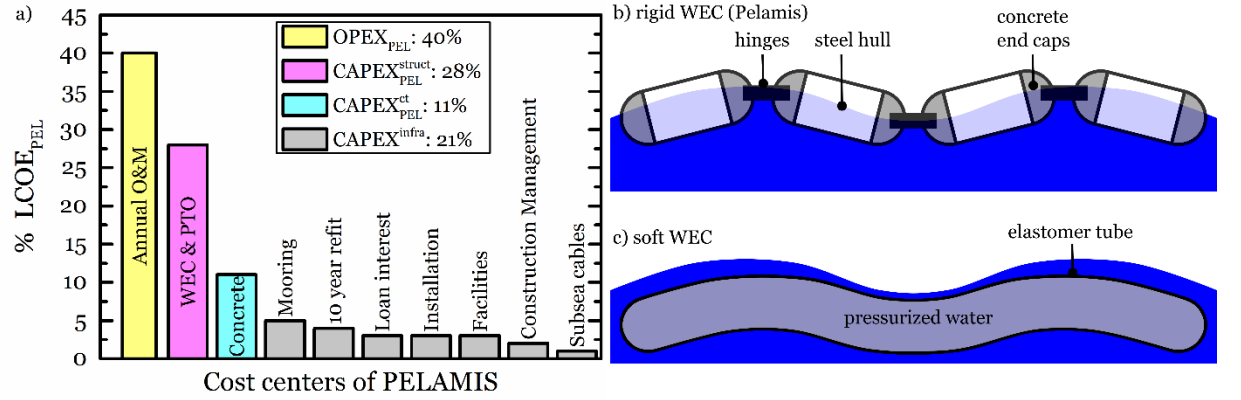

Supplementary Figure S2 | Cost centers of rigid wave energy converters (reproduced from data of McGowin et al. [16]) and schematics of soft and rigid WEC structure. a) The structural cost for the wave energy converter and power take off system (magenta) accounts for 28% of the LCOE and another 40% are caused by annual maintenance (yellow). b) The schematic structure of a rigid WEC (Pelamis) built from rigid tubes. The end caps of the tubes are connected by hinges which transmit the absorbed power to turbo-machinery and turbines. c) Schematic structure of a soft WEC with an entirely soft structure. No end caps and moving parts are needed. The elastomer tube itself is filled with pressurized water and can act as absorber and power take-off system when deformed by wave motion.

The cost centers defined in Previsic et al.[13] are combined into four categories

1. $CAPEX^{struct}_{PEL}$: (Levelized) Investement cost for construction and material of the wave energy converter itself including power take-off system and hull[16]. It accounts for $f_{struct} = 28\%$ of the total $LCOE_{PEL}$ of a Pelamis device.
2. $OPEX_{PEL}$: Annual cost for operation and maintenance including insurance, labor and parts[13]. This cost center does not include infrequent major overhauls. This cost center account for $f_{OPEX} = 40\%$ of the total $LCOE_{PEL}$.
3. $CAPEX^{infra}_{PEL}$: All (levelized) costs related to financing, management, installation of infrastructure needed to operate a wave energy converter or a farm of wave energy converters. Includes mooring, loan interest, installation, facilities, construction management, subsea cables and an overhaul of the WEC every 10 years. This cost center accounts for $f_{infra} = 21\%$ of the total $LCOE_{PEL}$.
4. $CAPEX_{PEL}^{ct}$: pretensioned concrete is used for the end caps connecting segments of a Pelamis wave energy converter and posttensioned concrete is coating the inside of the steel tube[18].

As no fuel is consumed by a WEC ($FUEL(t) = 0$) eq. S2 can be rewritten using these cost centers (note that the terms related to the discount rate r and lifetime T are now included in the CAPEX terms):

$$\mathrm{LCOE}_{\mathrm{PEL}} EGEN_{\mathrm{PEL}} = \mathrm{OPEX}_{\mathrm{PEL}} + \mathrm{CAPEX}^{\mathrm{struct}}_{\mathrm{PEL}} + \mathrm{CAPEX}^{\mathrm{infra}}_{\mathrm{PEL}} + \mathrm{CAPEX}^{\mathrm{ct}}_{\mathrm{PEL}} \quad (S3)$$

These four cost centers of Pelamis are analyzed and adjusted for differences to a soft WEC.
In the first step the $CAPEX^{PEL}_{struct}$ is split into two parts[19]: steel hull structure accounts for $f_{hull} = 35.4\%$ and power take-off system accounts for the rest of the structural cost.
The hull of a soft WEC operates as a device generating high voltage DC ready for long distance transmission, no PTOs are needed for generation and no AC-DC converter for transmission. The cost reduction due to savings regarding the PTO are unknown and to present a conservative estimation we include the full cost of PTOs as they appear in Pelamis.
In a second step the cost for the steel hull directly scales with the steel price per weight ($\$_{steel}$) and if replaced with an equal weight of elastomer ($\$_{soft}$) leads to (point 1):

$$\mathrm{CAPEX}^{\mathrm{struct}}_{\mathrm{soft}} = \mathrm{CAPEX}^{\mathrm{struct}}_{\mathrm{PEL}}\left(f_{\mathrm{hull}}\frac{\$_{\mathrm{soft}}}{\$_{\mathrm{steel}}} + \left(1 - f_{\mathrm{hull}}\right)\right) = f_{\mathrm{struct}}\left(f_{\mathrm{hull}}\frac{\$_{\mathrm{soft}}}{\$_{\mathrm{steel}}} + \left(1 - f_{\mathrm{hull}}\right)\right)\mathrm{LCOE}_{\mathrm{PEL}} EGEN_{\mathrm{PEL}} \quad (S4)$$

Lowering the cost of the initial structure also decreases maintenance costs.
Most of the maintenance for offshore WECs is due to four items[19]: insurance & taxes, unscheduled repairs after storms, preventive maintenance of PTO and turbines, scheduled subsystem replacements.
Storm damages can be reduced if soft WECs are deflated during such an event, a measure which is not possible for rigid WECs. In contrast to rigid WECs the soft WECs could be moved onto a ship because of their compliance, possibly allowing for preventive maintenance of multiple WECs simultaneously on one ship. Combining the reduction of storm damages and the easier handling of compliant structures with the low material price and the lack of turbines justifies the assumption of 20% cost reduction on $OPEX_{PEL}$ ($f_{red} = 0.8$) reduction considering a lifetime of 20 years for natural rubber tubes in sea as Pelamis (possible are up to 25 years according to Farley et al. [20]) compared to rigid WEC. The adjusted cost for operation and maintenance are given by

$$OPEX_{soft} = f_{\mathrm{red}} f_{\mathrm{OPEX}} \mathrm{LCOE}_{\mathrm{PEL}} EGEN_{\mathrm{PEL}} \quad (S5)$$

The cost for infrastructure, installation, management and connection of a WEC are not related to the type of WEC used. Thus $CAPEX^{PEL}_{infra}$ enters the LCOE of soft WECs without modification (point 3) and

$$\mathrm{CAPEX}_{\mathrm{infra}}^{\mathrm{soft}}(t) = \mathrm{CAPEX}_{\mathrm{infra}}^{\mathrm{PEL}}(t) = f_{\mathrm{infra}} \mathrm{LCOE}_{\mathrm{PEL}}\, EGEN_{\mathrm{PEL}} \qquad (S\,6)$$

Soft generators do not contain concrete end caps and to account for that the LCOE of soft WECs do not contain the cost for concrete (point 4) and thus.

$$\mathrm{CAPEX}_{\mathrm{ct}}^{\mathrm{soft}}(t) = 0 \qquad (S\,7)$$

The last modification refers to the energy generated by different devices. The measured maximum power density of soft generators ranges from $200\ kW/m^3$ (NR) to 280 $kW/m3$ (VHB[21]). These are maximum values from lab-scale experiments where the materials are operated at their limits. In real-world applications the materials will be operated at lower output values to increase the lifetime and reduce costs. For this reason only 1% of the maximum reported output power density ρ_{soft}^{max} is used as the average power density of a soft WEC where no average power density ρ_{soft}^{avg} is available from literature. We define the average power density by

$$\rho_{\mathrm{soft}} = \begin{cases} 1\%\ \text{of}\ \rho_{\mathrm{soft}}^{\max} & \text{for reported peak power densities} \\ \rho_{\mathrm{soft}}^{\mathrm{avg}} & \text{for reported avg power densities} \end{cases} \qquad (S\,8)$$

Since the same weight of hull material is used for calculating the $CAPEX_{soft}^{struct}$ we also use the same weight of material to calculate the produced energy

$$EGEN_{\mathrm{soft}} = \frac{EGEN_{\mathrm{PEL}}}{\rho_{\mathrm{PEL}}} \rho_{\mathrm{soft}} \qquad (S\,9)$$

Here the average power density of Pelamis ρ_{PEL} is calculated from reported values ($153\ kW$ average output power and mass of $380\ t$[16]) resulting in $\rho_{PEL} = 0.4\ mW/g$. Combining eq. S3-S9 we calculate the LCOE of a soft WEC as a function of material price $\$_{soft}$ and average power density ρ_{soft} with

$$\frac{\mathrm{LCOE}_{\mathrm{soft}}\left(\$_{\mathrm{soft}}, \rho_{\mathrm{soft}}\right)}{\mathrm{LCOE}_{\mathrm{PEL}}} = \frac{\rho_{\mathrm{PEL}}}{\rho_{\mathrm{soft}}} \left\{ f_{\mathrm{red}} f_{\mathrm{OPEX}} + f_{\mathrm{struct}} \left(f_{\mathrm{hull}} \frac{\$_{\mathrm{soft}}}{\$_{\mathrm{steel}}} + \left(1 - f_{\mathrm{hull}}\right) \right) + f_{\mathrm{infra}} \right\} \qquad (S\,10)$$

The price for manufactured steel was reported in 2004 to about $\$\ 3000/ton$[19] and accounting for increased raw steel price ($\$\ 650/ton$ (2004) to $\$\ 900/ton$ (2012)) the manufactured steel price per ton in December 2012 is $\$\ 4150/ton$. Elastomers used for soft WEC are VHB4910™ (VHB[22]: $\$\ 105000/ton$), silicone rubber (SR[23]: $\$\ 20000/ton$) and natural rubber (NR[20]: $\$\ 7600/ton$) .

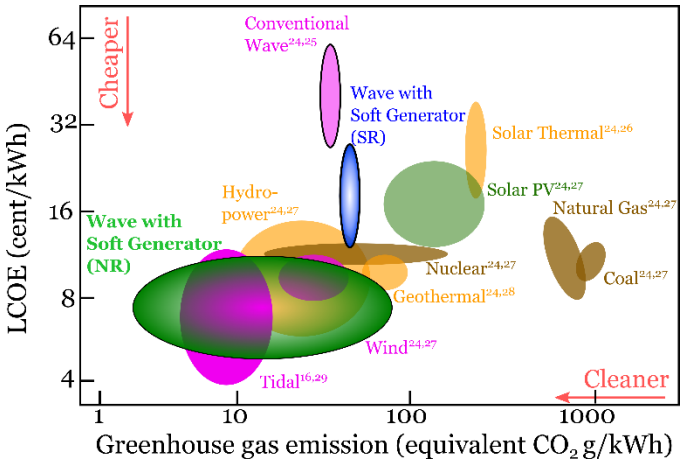

Supplementary Figure S3| LCOE and Greenhouse gas emissions of energy sources This chart shows that ocean wave energy harvesting is possible at low cost when soft DEGs made of NR are used. With renewable energy sources orders of magnitude less greenhouse gases are emitted at the same, or even lower price.[16,24–29]

Results for the LCOE using different elastomer materials in a soft WEC are listed in supplementary table S1.

Supplementary Table S1 | Comparison of the levelized cost of wave energy converters using different materials and technology. The first line (shaded) reports published LCOE for the Pelamis wave energy converter ($LCOE_{PEL}$)[30]. The following lines report estimates of $LCOE_{soft}$ for soft WECs using different materials calculated by eq. S10. The average specific power for natural rubber and VHB are estimated to be 1% of peak power in laboratory tests. The power of Pelamis and silicone rubber are reported in literature[16,17].

WEC	Average specific power ρ	Material cost \$	LCOE based on (cent/kWh) O'Connor 2013[30]
Pelamis (steel)	0.4 kW/ton [16]	\$ 4150/ton	26.5 – 61.7
Natural rubber	2 kW/ton	\$ 7600/ton	4.8 – 11.1
Silicone rubber	1.1 kW/ton [17]	\$ 20000/ton	11.8 – 27.5
VHB	2.8 kW/ton [31]	\$ 105000/ton	12.3 – 28.5

Soft WECs do not produce greenhouse gas (GHG) emissions during operation. For estimating the levelized emission of GHGs ($LGHG$) per generated electricity of soft WECs we only consider the emissions during production of the elastomer material (GHG) and its average power density (ρ_{soft}) but we exclude emissions during construction, installation, maintenance and decommissioning. According to Thomson et al. [32] most of the emissions of Pelamis are due to steel production and a similar situation should apply for soft WECs. The levelized emissions for soft WEC are therefore simplified by the following formula:

$$\mathrm{LGHG} = \frac{\mathrm{GHG}}{\rho_{\mathrm{soft}}\,\mathrm{Lifetime}_{\mathrm{soft}}} \qquad (\mathrm{S}\,11)$$

We assume equal lifetime of elastomers and steel in seawater (20 years) and consider the reported GHG emissions for NR (GHG of $0.54 - 21\ ton\ CO_2\ eq./ton$)[33] and silicone rubber (GHG of $6.3 - 6.6\ ton\ CO_2\ eq./ton$)[34]. The resulting LGHG for NR and silicone rubber are $1.5 - 60\ g\ CO_2\ eq./kWh$ and $33 - 34\ g\ CO_2\ eq./kWh$ respectively.

Depending on the source of natural rubber, from plants or from petrochemical reactions, the emissions vary considerably. The results are summarized in supplementary figure S3 and show that harvesting the energy of marine waves is cost-competitive and clean compared with other technologies. However the emissions caused by installation and infrastructure have not been considered in this estimation. All values regarding emissions of other techniques reported in literature include the emissions during construction, installation, operation and decommissioning.

Experimental Methods:

Deformation properties.

Material samples are tested with a ZWICK universal testing machine. The nominal stress (force divided by initial cross-sectional area) is recorded as a function of uniaxial stretch during loading and unloading.

Stress-stretch curves of pristine samples were obtained for a strain rate of 100%/s. The mechanical response of elastomers is fitted to the Gent model[35]. The Gent model consists of two material parameters: the shear modulus μ and a parameter J_{lim} that relates to the limiting stretch. The main text fig. 2b shows the experimentally-obtained uniaxial nominal stress-strain relation, fitted to the Gent model, giving material parameters μ, J_{lim} at a strain rate of 100%/s in the main text table 1.

Modeling the uniaxial deformation of the samples with the Gent model ($\lambda = \lambda_1; \lambda_2 = \lambda_3 = \lambda^{-0.5}$) gives the nominal stress s as a function of strain as follows:

$$s = \frac{\mu J_{lim}(\lambda^3 - 1)}{2\lambda - (3 + J_{lim})\lambda^2 + \lambda^4} \qquad (S\ 12)$$

Hysteresis.

When an elastomer undergoes a mechanical cycle of loading and unloading, the unloading path is typically different from its loading path. When plotted on a stress-strain plane, the resulting area traced by the loading-unloading cycle gives a measure of the amount of mechanical energy lost due to viscous effects, known as the hysteresis loss. We obtain hysteresis losses for samples of acrylic-based VHB, and natural rubber-based ZRU and OP, by an experiment of cyclic loading and unloading. Samples are uniaxially stretched to a prescribed maximum nominal strain of 200%, at a prescribed strain rate of 5%/s, and then unloaded at the same strain rate. This loading-unloading process was repeated 100 times for each sample. The 100th cycle is plotted in main text figure 2d-f) to illustrate the relative hysteresis losses for each material.

Hysteresis loss is expressed as a percentage of total mechanical energy stored during loading. The non-zero initial strain before loading indicates some residual strain in the material accumulated over previous cycles. This experiment shows that natural rubber-based ZRU and OP give lower hysteresis losses compared with acrylic-based VHB, with OP displaying the lowest loss at 2.3%.

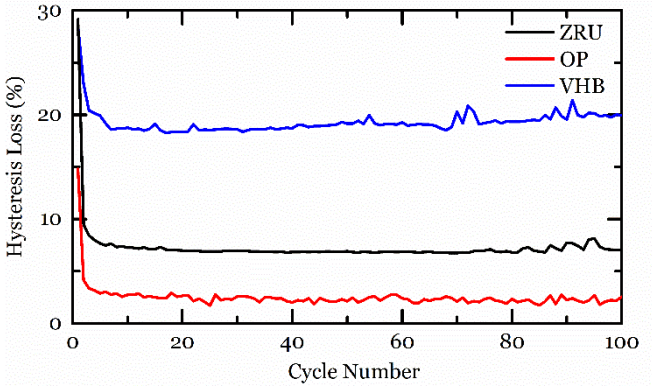

Supplementary Figure S4 | Evolution of the stress-strain hysteresis for VHB, ZRU and OP over 100 cycles of uniaxial loading-unloading. Consecutive cycles exhibit less and less hysteresis. After only 5 cycles the hysteresis loss converges toward its long term value.

All three materials exhibit large hysteresis losses in the first cycle, which gradually saturates to a lower value from the 5th cycle onwards (supplementary figure S4). This may be attributed to the Mullins effect[36,37] which is most observable in the first few stress cycles of a virgin elastomer, and gradually diminishes for subsequent cycles.

Fracture energy.

The fracture energy is defined as the mechanical energy required for a pre-existing crack to advance per unit area[38]. We determined the fracture energy of the elastomers by using an established method[38]. A wide but short sample of dimensions L and H was clamped along the long edge (inset on fig. 2c). A pristine sample and a sample with a precut were separately stretched in pure shear deformation mode. The fracture energy Γ is computed as:

$$\Gamma = W(\lambda_{rup}) \times H \qquad (S\ 13)$$

where λ_{rup} denotes the rupture stretch of the precut sample. The mechanical energy density $W(\lambda)$ is obtained from the area under the measured nominal stress-stretch curve of a pristine sample. The data obtained were put into equation (S13), and the fracture energies for all elastomers were summarized in main text table 1.

Dielectric strength.

The intrinsic dielectric strength is obtained by a method previously suggested by Tröls et al.[39]. The dielectric strength is the maximum field applied to small area electrodes ($0.25mm^2$) separated by the elastomers thickness while ramping up the voltage until breakdown. A large flat stamp is pressed to the surface of the sample to prevent any actuation due to the applied voltage.

Dielectric permittivity.

The dielectric permittivity is measured with an impedance spectrometer (NOVOCONTROL with Alpha-A analyzer). This measurement reveals the polarizability (real part of permittivity ε) and the dielectric losses during polarization (e.g. through current leakage, series resistance and dissipative processes) which are represented by $\tan\delta$. The result of such spectroscopy is shown in supplementary figure S5.

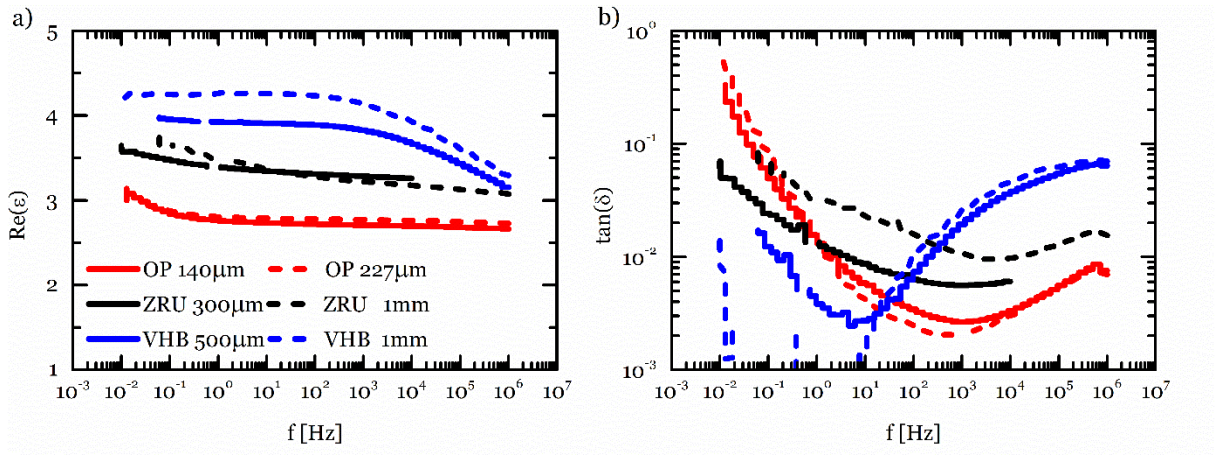

Supplementary Figure S5 | Thickness independence of dielectric properties of OP, ZRU and VHB. a) The polarizability of VHB, OP and ZRU is about $Re(\varepsilon) \approx 3$ over the whole frequency range, slightly increases for very low frequency. b) The loss tangent $\tan\delta$ is below 1 for the whole measurement range which indicates that loss mechanisms such as current leakage do not dominate the system and hence the material is suitable as a dielectric for a capacitor.

Since the observed dielectric properties are independent of thickness it is expected, that the intensive quantities specific energy and specific power are indeed thickness independent and non-linear effects can be neglected as long as the time to complete a generation cycle is small compared to the storage time of the capacitor which can be estimated to $t_{\text{store}} \approx (2\pi f \tan\delta)^{-1}$. For signals of $f = 1\ \text{Hz}$ this evaluates to $t_{\text{store}} \approx 10\ \text{s} - 100\ \text{s}$.

Analysis of filler content of the samples.

The commercially available rubber samples OppoBand 8003 and ZruElast A1040 were analyzed for their filler content by thermal gravimetric analysis (TGA). The samples are heated at a rate of $20\ °C/s$ from room temperature up to $600\ °C$ in nitrogen atmosphere to break down the polymer chains which evaporate. This stage is followed by adding oxygen to the atmosphere in the furnace which results in exothermal combustion of the carbon content of the sample. All organic components of the sample are oxidized after this process and further increase of the temperature to $800\ °C$ now oxidizes inorganic material. The remains of the sample are non-oxidized inorganic compounds. Supplementary figure S6 presents the analysis of OP and ZRU.

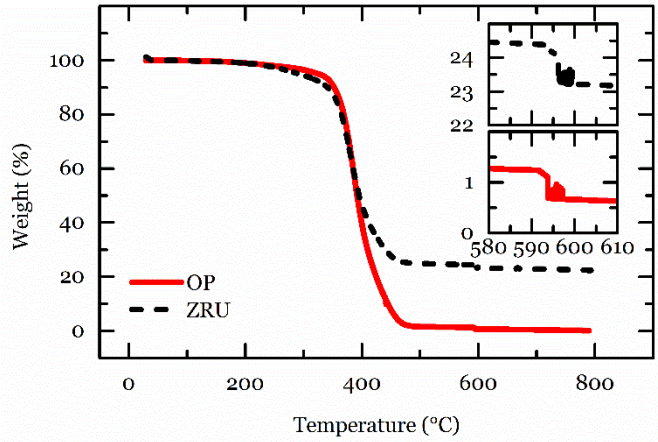

Supplementary Figure S6 | Thermal gravimetric analysis of OP and ZRU. The bulk of the rubber material is broken down at about $400\ °C$ in a nitrogen atmosphere, leaving only the filler materials on the precision scale. The following injection of oxygen at about $600\ °C$ leads to combustion of the carbon content (zoomed out in the insets). The remains after this process are inorganic compounds which do not oxidize up to 800°C.

The filler content of OP is: $0.56\ \%$ carbon, $0.96\ \%$ inorganic compounds. The filler content of ZRU is: $1.19\ \%$ carbon and $23\ \%$ inorganic compounds. The high filler content of ZRU may be the cause of the pronounced Mullins effect seen in supplementary figure S4.

Material assessment in soft generators.

A sample membrane with diameter of $3\ cm$ is mounted onto a pressure chamber. Pressure and volume inside the inflated membrane are measured by a pressure sensor (JUMO dTrans p30 40.4366) and a high-speed camera at $250\ fps$ (JVC GC-PX10). A contactless voltage measurement is performed by a TREK 341A electrostatic voltmeter to obtain the voltage at the membrane. The voltage drop/rise during charging/discharging the membrane is used to determine the charges $Q_{in/out}$ exchanged with the input/output charge reservoirs (two $440\ nF$ high-voltage capacitors from www.fjz-ajf.de). The high-voltage diodes used for directing the charge exchange are X100UFG.

References

1. Solomon, S. et al. IPCC, 2007: Climate Change 2007: The Physical Science Basis. Contribution of Working Group I to the Fourth Assessment Report of the Intergovernmental Panel on Climate Change. D Qin M Manning Z Chen M Marquis K Averyt M Tignor HL Mill. New York Cambridge Univ. Press pp **Geneva,** 996 (Cambridge University Press, 2007).
2. Chu, S. & Majumdar, A. Opportunities and challenges for a sustainable energy future. Nature **488,** 294–303 (2012).
3. Hagerman, G. & Scott, G. Mapping and Assessment of the United States Ocean Wave Energy Resource 2011. (EPRI, 2011).
4. OES/IEA. Ocean Energy Systems: Annual Report 2011. (OES/International Energy Agency, 2011).
5. OES/IEA. Ocean Energy Systems: Annual Report 2007. (OES/International Energy Agency, 2007).
6. Ummel, K. & Wheeler, D. Desert Power: The Economics of Solar Thermal Electricity for Europe , North Africa , and the Middle East. (2008). doi:dx.doi.org/10.2139/ssrn.1321842

7. Dickson, M. H. & Fanelli, M. Report of the IGA to the UN Commission on Sustainable Development, Session 9 (CSD-9): Contribution of Geothermal Energy to Sustainable Development. (2004). at <http://www.geothermal-energy.org/geothermal_energy/what_is_geothermal_energy.html>
8. Holm, A., Blodgett, L., Jennejohn, D. & Gawell, K. Geothermal Energy: International Market Update May 2010. 4–6 (International Geothermal Energy Association, 2010). at <http://www.geo-energy.org/pdf/reports/gea_international_market_report_final_may_2010.pdf>
9. Jacobson, M. Z. & Archer, C. L. Saturation wind power potential and its implications for wind energy. Proc. Natl. Acad. Sci. U. S. A. **109,** 15679–84 (2012).
10. Worldwide electricity production from renewable resources: Fourteenth Inventory Edition 2012. (Observ'ER, 2012). at <http://www.energies-renouvelables.org/observ-er/html/inventaire/pdf/14e-inventaire-Chap02.pdf>
11. Photovoltaic Barometer. 108–131 (EurObserv'ER, 2012).
12. Renewable Energy Essentials: Hydropower. (OECD/IEA, 2010).
13. Previsic, M., Siddiqui, O. & Bedard, R. E2I EPRI WP - US --002 Rev 4: Economic Assessment Methodology for Offshore Wave Power Plants. (EPRI, 2004).
14. Hardisty, J. The Analysis of Tidal Stream Power. (John Wiley & Sons, Ltd, 2009). doi:10.1002/9780470743119
15. Bedard, R. et al. E2I EPRI Global WP 009 - US Rev2: Offshore Wave Power Feasibility Demonstration Project. 34 (EPRI, 2005).
16. McGowin, C. et al. Renewable Energy Technical Assessment Guide —TAG-RE: 2006. EPRI. **3,** (EPRI, 2007).
17. Jean, P. et al. Standing wave tube electro active polymer wave energy converter. in Proc. SPIE 83400C–83400C–21 (2012). doi:10.1117/12.934222
18. Anderson, C. Pelamis WEC - Main Body Structural Desgin and Materials Selection. (DTI New and Renewable Energy Programme, 2003). at <http://webarchive.nationalarchives.gov.uk/+/http://www.dti.gov.uk/energy/renewables/publications/pdfs/v0600197.pdf>
19. Previsic, M., Bedard, R., George, H. & Siddiqui, O. E2I EPRI Global - 006A - SF: System Level Design , Performance and Costs for San Francisco California Pelamis Offshore Wave Power Plant. 73 (EPRI, 2004).
20. Farley, F. J. M., Rainey, R. C. T. & Chaplin, J. R. Rubber tubes in the sea. Philos. Trans. A. Math. Phys. Eng. Sci. **370,** 381–402 (2012).
21. Huang, J., Shian, S., Suo, Z. & Clarke, D. R. Maximizing the Energy Density of Dielectric Elastomer Generators Using Equi-Biaxial Loading. Adv. Funct. Mater. n/a–n/a (2013). doi:10.1002/adfm.201300402
22. 3M. Webshop 3M™ for VHB™ Tape 4910 Clear, 12 in x 36 yd 40.0 mil: $1089.48/Roll. (2013). at <www.shop3m.com>
23. Rubber-Cal Inc. Premium Grade Silicone Rubber Sheet with Higher Physical Properties. at <http://www.rubbercal.com/Silicone_PG.html>
24. Levelized Cost of New Generation Resources in the Annual Energy Outlook 2012. Annu. Energy Outlook 2012 (Energy Information Administration, 2012).
25. Parker, R. P. M., Harrison, G. P. & Chick, J. P. Energy and carbon audit of an offshore wave energy converter. Proc. Inst. Mech. Eng. Part A J. Power Energy **221,** 1119–1130 (2007).
26. Lechón, Y., de la Rúa, C. & Sáez, R. Life Cycle Environmental Impacts of Electricity Production by Solarthermal Power Plants in Spain. J. Sol. Energy Eng. **130,** 021012 (2008).
27. Lenzen, M. Life-Cycle Energy Balance and Greenhouse Gas Emissions of Nuclear Energy: A review. Energy Convers. Manag. **49,** 2178–2199 (2008).
28. Frick, S., Kaltschmitt, M. & Schröder, G. Life cycle assessment of geothermal binary power plants using enhanced low-temperature reservoirs. Energy **35,** 2281–2294 (2010).
29. Kelly, K. A., McManus, M. C. & Hammond, G. P. An energy and carbon life cycle assessment of tidal power case study: The proposed Cardiff–Weston severn barrage scheme. Energy **44,** 692–701 (2012).
30. O'Connor, M., Lewis, T. & Dalton, G. Techno-economic performance of the Pelamis P1 and Wavestar at different ratings and various locations in Europe. Renew. Energy **50,** 889–900 (2013).
31. Kaltseis, R. et al. Method for measuring energy generation and efficiency of dielectric elastomer generators. Appl. Phys. Lett. **99,** 162904 (2011).
32. Thomson, R. C., Harrison, G. P. & Chick, J. P. Full life cycle assessment of a wave energy converter. IET Conf. Renew. Power Gener. (RPG 2011) 63–63 (2011). doi:10.1049/cp.2011.0124
33. Jawjit, W., Kroeze, C. & Rattanapan, S. Greenhouse gas emissions from rubber industry in Thailand. J. Clean. Prod. **18,** 403–411 (2010).
34. Brandt, B., Kletzer, E., Pilz, H., Hadzhiyska, D. & Seizov, P. Silicone-Chemistry Carbon Balance. 1–58 (Global Silicones Council, 2012).
35. Gent, A. N. A New Constitutive Relation for Rubber. Rubber Chem. Technol. **69,** 59–61 (1996).
36. Bueche, F. Molecular basis for the mullins effect. J. Appl. Polym. Sci. **4,** 107–114 (1960).

37. Dorfmann, A. & Ogden, R. W. A constitutive model for the Mullins effect with permanent set in particle-reinforced rubber. Int. J. Solids Struct. **41,** 1855–1878 (2004).
38. Pharr, M., Sun, J.-Y. & Suo, Z. Rupture of a highly stretchable acrylic dielectric elastomer. J. Appl. Phys. **111,** 104114 (2012).
39. Tröls, A. et al. Stretch dependence of the electrical breakdown strength and dielectric constant of dielectric elastomers. Smart Mater. Struct. **22,** 104012 (2013).